

Changes in the fluorescence of the Caribbean coral *Montastraea faveolata* during heat-induced bleaching

David G. Zawada¹ and Jules S. Jaffe

Scripps Institution of Oceanography, 9500 Gilman Drive, La Jolla, California 92093-0238

Abstract

In order to evaluate the response of commonly occurring green and orange fluorescent host-based pigments, a thermal stress experiment was performed on specimens of the Caribbean coral *Montastraea faveolata*. Seven paired samples were collected from a small oceanic reef near Lee Stocking Island in the Bahamas. Seven of the fourteen corals were subjected to elevated temperatures for 28 d, followed by a recovery period lasting 53 d. Throughout the experiment, high-resolution ($\sim 400 \mu\text{m pixel}^{-1}$) multispectral images of induced fluorescence were recorded at wavelengths corresponding to the green and orange host pigments, plus chlorophyll. These images revealed that the fluorescence of both host pigments was concentrated at polyp centers and declined by 70–90% in regions between polyps. Chlorophyll fluorescence, however, was distributed almost uniformly across the entire coral surface, but with decreases of 10–30% around polyp centers. A normalized difference ratio between the green and orange pigments (GO ratio) was developed to facilitate comparison with chlorophyll fluorescence as a bleaching indicator. Analysis showed a high correspondence between a sustained GO ratio of less than zero and the death of corals. Finally, this ratio was resistant to contamination from other sources of chlorophyll fluorescence, such as filamentous algae.

Beginning with the work of Kautsky and Hirsch (1931), induced chlorophyll fluorescence has been used to gain a better understanding of the photosynthetic apparatus in plants. Mohammed et al. (1995) and Lazar (1999) provide recent reviews of relevant techniques and required instrumentation. Expanding on these methods, induced fluorescence from photosynthetic pigments has long been used to investigate the physiological state, spatial distribution, and other characteristics associated with phytoplankton (Lorenzen 1966; Oneill et al. 1975).

Owing to their dinoflagellate symbionts, collectively referred to as zooxanthellae, hermatypic (reef-building) corals also contain photosynthetic pigments (Jeffrey and Haxo 1968). Corals, moreover, often contain additional fluorescent pigments in their animal tissue (Kawaguti 1944; Limbaugh and North 1956; Catala 1959; Shibata 1969; Mazel 1995) whose ecological significance is under current investigation. Using both the benthic spectrofluorometer (BSF), a submersible handheld spectrometer/fluorometer, and a laboratory-based spectrofluorometer, Mazel (1997a,b) measured the reflectance and fluorescence spectra in situ from several hundred Caribbean coral specimens. Analysis of the data revealed that combinations of four pigments accounted for the majority of observed fluorescent colors. Based on the ap-

proximate location of their emission peak, these pigments were designated as 486, 515, 575, and 685. The first three pigments are contained in the ectodermal tissue, while 685 (chlorophyll) is attributable to the symbiotic dinoflagellates that are found in the endoderm (Kawaguti 1944; Mazel 1995).

The function of the host-based pigments remains an open question. It has been suggested that they provide photoprotection (Kawaguti 1944) by absorbing potentially damaging short wavelength radiation and dissipating the energy at longer wavelengths via fluorescence. Another theory ascribes a photosynthetic enhancing role to the pigments (Kawaguti 1969, 1973), under the supposition that the fluoresced light is reabsorbed by the light harvesting apparatus of the symbiotic dinoflagellates. Recent work has attempted to substantiate both hypotheses, but the results are inconclusive. Salih et al. (1997) investigated fluorescent pigments of corals collected in both the Great Barrier Reef and the Red Sea from 1–5-m and 10–22-m depth ranges. Fluorescence microscopy was used to observe the response of the specimens to excitation at 365, 395–440, and 450–490 nm. Subjectively, the 395–440 nm excitation was reported as producing the strongest fluorescent response, followed by that at 450–490 nm and 365 nm. Further microscopic analysis revealed a pattern in the distribution of the pigments. In corals taken from 1–5-m depths, the fluorescent pigments were located in the ectoderm and outer parts of the endoderm, primarily above the symbiotic dinoflagellates. Conversely, in corals collected deeper, the pigments were found to be concentrated beneath and/or among the symbiotic dinoflagellates. Based on these qualitative observations, the authors suggested that fluorescent pigments provide UVA/blue radiation protection for corals living in high light habitats and enhance photosynthetic output for corals residing in low-light habitats. In another study, Salih et al. (2000) concluded that in excessive sunlight, fluorescent pigments function as photoprotectants for both the symbiotic dinoflagellates and sensitive coral tis-

¹ Current address: WET Labs Inc., 620 Applegate St., Philomath, Oregon 97370 (davez@mpl.ucsd.edu).

Acknowledgments

The authors thank the Office of Naval Research–Environmental Optics Program and the Achievement Rewards for College Scientists (ARCS) Fellowship for funding this research. Ben Ochoa provided much appreciated engineering support. The manuscript was greatly improved by the insightful comments and suggestions of Nancy Knowlton, Wes Toller, Charlie Mazel, Gisèle Muller-Parker, Peter Franks, and an anonymous reviewer. We also thank Nancy Knowlton for the use of her wet lab, as well as Wes Toller for genotyping the symbiotic dinoflagellates from our coral specimens.

sues by absorbing ultraviolet-A (UVA) radiation. However, if a given fluorescent substance protects against UVA radiation by absorption, one would expect to find a corresponding peak in this region of the excitation spectrum. Aside from a single blue fluorescent pigment in *Acropora nobilis*, none of the pigments mentioned in their study were shown to have excitation peaks in this waveband. Similar UVA-absorbing, blue fluorescent pigments also have been found in other acroporid corals, as well as in *Pocillopora damicornis* (Dove et al. 2001).

Photosynthetic enhancement in typically deep-water species by fluorescent host pigments also has been suggested by Schlichter et al. (1986, 1994). In these species, pigment granules were located beneath the symbiotic dinoflagellates. Chloroform extracts containing these pigments were found to absorb between 380 and 400 nm and fluoresce between 440 and 550 nm, a waveband of light that could be absorbed by the photosynthetic apparatus of the symbiotic dinoflagellates. As pointed out by Mazel (1995), these findings are not applicable to corals in general because the fluorescent compounds in question are located beneath the symbiotic dinoflagellates, not above them in the ectodermal tissues as reported by others, and the corals contain additional structural adaptations. One should also consider the fact that the pigment analyses were performed on extracts. In vivo analysis could lead to different spectral responses.

One aspect of the fluorescent host pigments that has not been addressed is their potential use as health indices. Myers et al. (1999) demonstrated that these signals can be used to distinguish between pigmented and bleached corals and between coral and macroalgae. Additionally, they speculated on the potential of using these fluorescent signals for assessing reef health from remote sensing platforms. We extend this effort by monitoring the fluorescence changes of the 515, 575, and 685 pigments throughout the bleaching process.

Coral bleaching is often defined as the loss of algal symbionts and/or a decrease in their photosynthetic pigment concentrations (Porter et al. 1989; Fitt and Warner 1995; Glynn 1996; Brown 1997b). Several environmental stressors have been linked to bleaching events, including elevated sea temperatures, increased solar radiation, decreased salinity, and sedimentation (see reviews by Glynn 1993 and Brown 1997b). Using pulsed-laser spectroscopy, Hardy et al. (1992) documented a dramatic decline in chlorophyll fluorescence from seven different Caribbean coral species as they bleached in response to a constant thermal stress over a 5-d period. Similarly, bleaching was induced in this study by only applying a thermal stress to specimens of the Caribbean coral *Montastraea faveolata*. Using chlorophyll fluorescence as a bleaching indicator, we simultaneously recorded two-dimensional images of 515 and 575 fluorescence to investigate possible manifestations of stress associated with these host-based pigments.

Materials and methods

Coral collection and handling—In June 1999, seven specimens of *M. faveolata* were collected from seven different

colonies on a small oceanic reef north of White Horse Cay (near Lee Stocking Island), Bahamas (23°48.3'N, 76°8.7'W), at a depth of 7–11 m. Using a hammer and chisel, samples approximately 20 × 10 cm in size were chipped off the upward facing edges of the coral heads. To facilitate a paired sampling technique, the samples were broken into roughly 10 × 10-cm halves in the field and placed in separate zip-lock plastic bags. Approximately 12 h after collection, the corals were prepared for transport to the Scripps Institution of Oceanography (La Jolla, California) using a dry shipping method (Delbeek and Sprung 1994). Upon arrival, the corals were immediately taken to a specially configured wet lab and distributed among six 20-liter aquaria. No more than three specimens were placed in any given aquarium. Filtered (>20 μm) and heated seawater was continuously supplied to each aquarium at a rate of approximately 12.5 ml s⁻¹. The water temperature was maintained between 25.5 and 27°C. Each aquarium was also continuously aerated via air stones. Air temperature in the lab was kept in the range of 24–28°C. To control algal growth, marine snails (*Turbo fluctuosus*) were placed in the aquaria. Natural sunlight was mimicked by placing two 40 W VitaLights above each set of three aquaria. The lights were controlled by a timer set to a 14:10 light:dark (LD) cycle. Incident scalar irradiance, integrated from 400 to 700 nm, at the coral surfaces was 37 μmol quanta m⁻² s⁻¹. After traveling in total darkness for approximately 10 h, light shock was a concern. Therefore, a double layer of window screening was draped over all of the aquaria. After 24 h, one layer was removed. After an additional 48 h, the second layer was removed. The corals were left to adapt to their new habitat for a period of 3 weeks. During this time, tissue samples were taken so that the symbiotic dinoflagellates could be extracted and genotyped according to the method of Rowan and Powers (1991). After the acclimation period, all coral specimens were alive and exhibited no signs of bleaching. To facilitate further handling, each coral was mounted on a PVC plastic disc (9-cm diameter × 5-cm high) with Hold Fast Epoxy Stick™ by Aquarium Systems.

Temperature regulation—The 14 coral halves were separated into control and treatment groups, such that each of the seven specimens constituted a control–treatment pair. The control group was maintained between 25.5 and 27°C. Data obtained from the Caribbean Marine Science Center indicate that in a typical year water temperatures at White Horse Cay fall in the range of 26–28°C. Submersible water heaters were placed in each of the treatment aquaria. At the start of the experiment, the water temperature in the treatment aquaria was increased 1°C every 2 h until a temperature of 31°C was reached. After 21 d at 31°C, the temperature was gradually increased to 34°C and maintained for seven more days. Over the following 48 h, the treatment water temperature was gradually returned to the same temperature as the control group and kept at that level for the remainder of the experiment.

Experimental apparatus—To capture fluorescence images, we used the Low-light-level Underwater Multispectral Imaging System (LUMIS). This instrument combines a scien-

Table 1. Passband characteristics of the interference filter set.

Central wavelength (nm)	Bandwidth (FWHM)	Transmission (%T)
460.2	42.1	58.0
521.7	12.0	78.0
582.2	17.3	86.5
678.3	22.0	84.0

tific-grade CCD camera (Medoptics K1000 from Medoptics Corporation) with an optical splitter (MultiSpec Imager™ from Optical Insights), which allows simultaneous imaging over four discrete spectral bands. The Medoptics K1000 camera uses a front-illuminated, full-frame Kodak KAF-1000 CCD. The considerable size (24.6×24.6 mm spanned by 1024×1024 pixels) of this detector provides large ($24 \times 24 \mu\text{m}$) photosensitive pixels. Complemented by a sizable photon storage capacity ($141,000$ electrons pixel^{-1}), these features enhance the suitability of this CCD for low-light applications. The CCD also possesses a wide dynamic range (14 bits pixel^{-1}) and uses both thermoelectric cooling and multipinned phase operation to minimize dark current generation (≤ 1 electrons $\text{pixel}^{-1} \text{ s}^{-1}$ at -25°C). Pixel values are in units of digital numbers (DN). The number of incident photoelectrons comprising 1 DN depends on the system gain. For LUMIS, nine photoelectrons are required to register 1 DN in a given pixel.

The MultiSpec Imager™ is a compact cylindrical device (6.7-cm diameter \times 14-cm long) that transforms an image from a single collection lens into four identical copies and projects each one onto a different quadrant of a single focal plane, which for LUMIS is the CCD. By installing an array of 25.4-mm filters, each quadrant can capture a discrete waveband. This set of filters is easily changed by the user. The MultiSpec Imager™ attaches to the Medoptics camera with a standard Nikkor F-mount bayonet. The collection end of the device accepts C-mount lenses in either 2/3 or 1 inch formats. LUMIS uses a 12.5-mm focal length, 1 inch format Computar lens. This lens provides a 18×18 -cm field of view at a target distance of 43 cm. With this configuration, the spatial resolution of an image is approximately $400 \mu\text{m}$ pixel^{-1} . Although the lens has a maximum aperture of $f/1.3$, the optics within the MultiSpec Imager™ have an effective maximum aperture of $f/2.8$.

Coral fluorescence was induced by a 4-ms excitation flash from a 400 J xenon strobe (Norlite 400 from Normark) equipped with a UV-blocked flash tube. Strobe output was restricted to blue light (~ 460 nm) with an interference filter. The pigments of interest in this study fluoresce green (~ 515 nm), orange (~ 575 nm), and red (~ 685 nm). Accordingly, LUMIS was fitted with custom-made interference filters (Intor, Inc., Sorocco, New Mexico) to simultaneously record each of these emissions in three of its four available spectral bands. The remaining band had a spectrally identical filter to the one used with the strobe to record blue light reflected from the surface of the corals. The passband characteristics of all the filters are provided in Table 1. To avoid signal contamination, the filters were constructed with nonfluoresc-

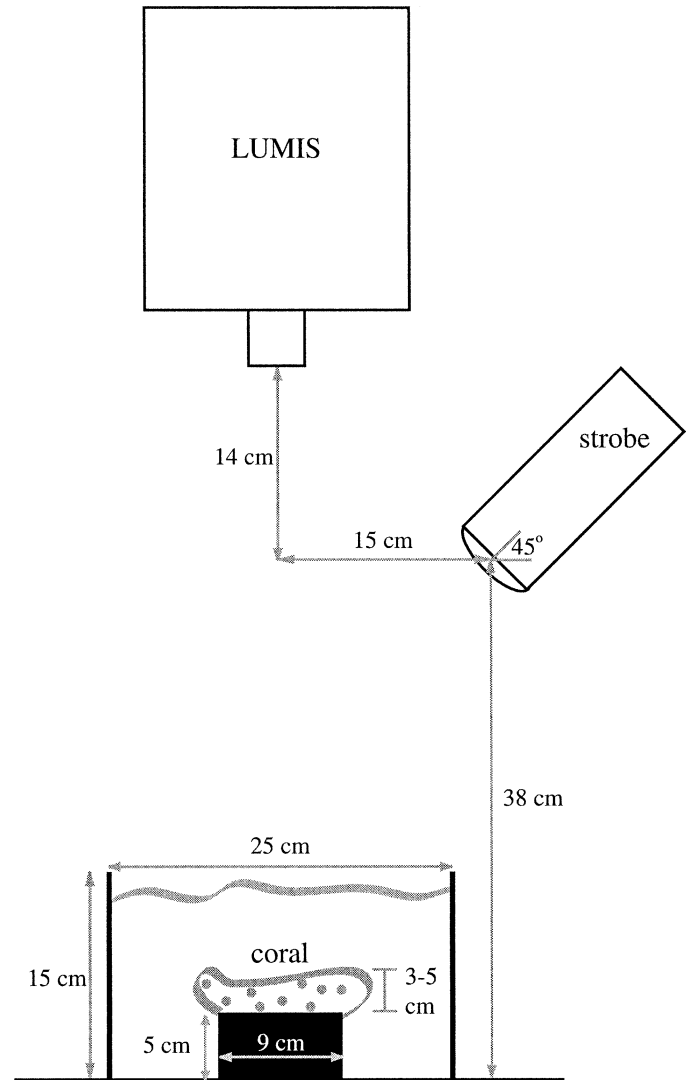


Fig. 1. Experimental setup. The coral specimens were glued to PVC disks to facilitate handling without touching the living tissue. To reproduce the same orientation of each specimen beneath LUMIS, holes were drilled in the bottom of the disks that aligned with pegs fixed to the bottom of the water bath.

ing materials. Owing to the high sensitivity of the CCD, the filters also had to strongly reject photons outside of the passband. The off-band blocking of these filters allows no more than 0.001% transmission.

To preclude the fluorescent signals being compromised by ambient light, all images were collected in the dark. A temporary darkroom was constructed by securing LUMIS in a stand with the camera looking straight down and wrapping the entire apparatus with a double layer of black felt (Fig. 1). A PVC dish (25-cm diameter, 15-cm deep) was centered and glued beneath the collection lens of LUMIS. This dish was used to hold a given coral specimen while it was being imaged. To ensure repeated placement of each coral in the same orientation beneath LUMIS, three steel pegs were mounted in the bottom of the dish to mate with holes in the PVC discs holding the corals. Prior to imaging, the dish was

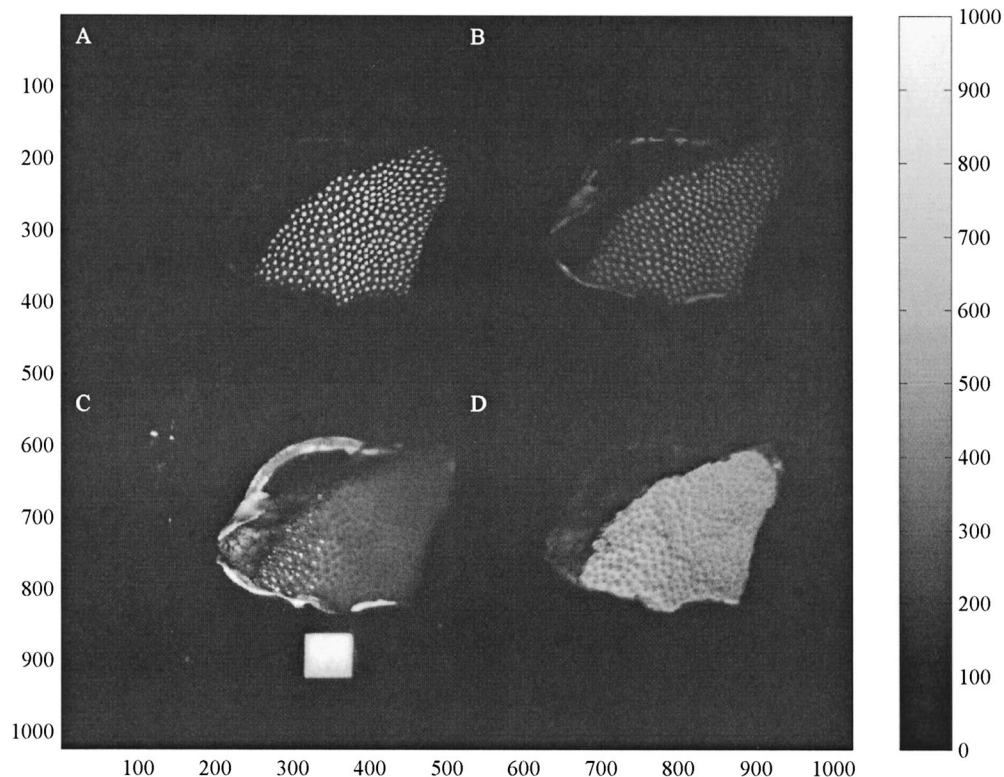


Fig. 2. Raw LUMIS image. Each 512×512 pixel quadrant represents a different spectral waveband: (A) 515 nm, (B) 575 nm, (C) 460 nm, (D) 685 nm. The square at the bottom of quadrant C is an opaque white plastic tile used for calibration purposes. Pixel values are in digital numbers proportional to the number of photons collected by the CCD at a given pixel. The stronger the fluorescent emission, the higher the recorded digital number.

filled with seawater taken from the aquaria. To avoid thermal shock, the water was changed between imaging the control and treatment corals.

It should be noted that the focus of this experiment was to monitor the relative changes in coral fluorescence in response to thermal stress. A secondary goal was to evaluate the feasibility of using a broadband sensor for this type of exercise. No attempt was made to ascertain the absolute number of photons emitted in the wave bands under consideration. Accordingly, LUMIS was not radiometrically calibrated. Also, note that the quantum efficiency of a CCD is a function of wavelength and can vary from one CCD to another. The data in this study were not normalized to account for differences in spectral sensitivity. If this experiment were repeated with another camera system, the magnitude of the results would likely be different. However, the observed patterns and relative changes in fluorescence would be the same. Fluorescence is also a function of the excitation wavelength and intensity.

Image collection—For the first 28 d of the experiment, images of coral fluorescence were taken every morning and evening, at approximately 0900 and 1700 h. During this period of time, the treatment group was subjected to sustained elevated temperatures, including 7 d at 34°C . For the remaining 53 d of the experiment, images were taken on a weekly basis, resulting in 72 sample points for each coral

for the entire experiment. An imaging session involved placing individual corals in the dish and collecting five sets of images. Each set consisted of a 10-ms exposure to record fluorescence, bracketed by 10-ms dark current images. The latter were used to develop an accurate model of the CCD dark current. No observations were made regarding the expansion/retraction of coral polyps during the imaging sessions.

Image correction—The data set for this experiment consists of over 15,000 LUMIS images that are $1,024 \times 1,024$ pixels and 2 MB in size. Each raw LUMIS image is composed of four distinct images (Fig. 2), one for each spectral band. Prior to performing any analysis, a number of preprocessing steps were completed. The first step was to remove the dark current component of the images. To a CCD, visible light and thermal radiation are indistinguishable energy sources and result in the accumulation of charge. The raw images, therefore, contain erroneously high pixel intensities. Once quantified, the dark current component can be subtracted from pixel values. To characterize the dark current uniformity of the CCD in LUMIS, a set of 111 dark images was collected over an 8-d period. Subsequent analysis revealed a consistently stable response across the entire chip, as quantified by a standard deviation of less than 1 DN for dark values on the order of 160 DN. Furthermore, the range of dark current values conformed to a normal distribution.

Both of these findings are expected from high quality, scientific-grade CCDs. Statistical analysis of dark current images showed that the mean pixel value serves as the maximum likelihood estimator for the true dark current. Since every fluorescence image was flanked by dark current images, the average pixel value over these two images was used as the dark current correction factor and subtracted from every pixel in the corresponding LUMIS image. After applying the dark current correction, each set of five LUMIS images was averaged to yield one corrected image per coral per sample time in the series. Inter-image variability was evaluated by computing the ratio of the standard deviation to the mean for corresponding pixels in each set of five images. Ratio values ranged from 0.004 to 0.02, indicating an inter-image variability from 0.4% to 2.0%.

The next step was to separate each of the averaged, dark-corrected LUMIS images into four separate images, one for each recorded spectral band. Since the corals varied in both size and shape, the individual spectral band images were cropped to exclude nonessential portions of the images, thereby reducing both computational and storage needs.

Finally, the images were geometrically corrected to rectify nonlinear distortions introduced by the Optical Insights MultiSpec Imager™. For each coral, the 575 nm fluorescence image from the initial sample time was used as the reference. All of the remaining images from all wave bands were warped to bring them into registration with the initial 575 nm image on a per coral basis. The warping was performed by an algorithm based on Delaunay triangulation and bicubic interpolation (Green et al. 1975).

Image processing—Initial inspection of the corrected images revealed that both the 515 and 575 nm signals emanated from the polyp centers and that fluorescence values rapidly decreased toward zero in the space between polyps. Chlorophyll (685 nm) fluorescence, however, was rather evenly distributed across the surface of the coral, except at the polyp centers, where its intensity declined. To improve the signal-to-noise ratio, pixels associated with polyp centers were extracted from all of the 515 and 575 nm images and used in further analysis. Given the sharp contrast in these images, a dynamic global thresholding algorithm was used to isolate polyp center pixels.

At each sample time, the relevant pixel values were averaged, yielding a representative fluorescence value for each LUMIS waveband. This procedure produced three time series (one per fluorescent pigment) for each of the control and treatment corals. The time series contain 72 data points, two for each sample day of the experiment. Initial inspection of the chlorophyll fluorescence curves (Figs. 5 and 6, 685 nm column) for both the control and treatment corals revealed that the first two data points consistently had a significantly larger magnitude than the remaining 70 points. The cause is unknown. Since these data were collected on day one of the experiment, perhaps the drop is attributable to the initial handling of the corals. Since this pattern was consistent in all of the time series, these first two points were excluded from further analysis of all three pigments. For each data point, the corresponding 99% confidence interval was computed and plotted along with the time series. Each element of the

time series is the average of several hundred to a few thousand pixel values. There is a 99% probability that the true mean value lies within the stated interval (Zar 1999).

GO ratio—In analyzing multispectral imagery, a frequent goal is to distill the multiple values per pixel into a single number that preserves the essence of the discrete spectral bands at each pixel. Researchers in the agricultural sciences were among the first to develop such techniques. Since the early 1970s, numerous indices have been devised to assess the state of a vegetative canopy from imagery acquired by remote sensing instruments, such as the Landsat multispectral scanner (Perry and Lautenschlager 1984). The most straightforward example is the band ratio, computed by dividing one spectral band by another on a pixel-wise basis. The benefits of band ratios include the removal of scene illumination effects, suppression of surface albedo differences, and the enhancement of subtle spectral variations (Lillesand and Kiefer 1994).

To investigate the interrelationship between 515 nm (green) and 575 nm (orange) fluorescence, a variant of the standard band ratio was used, known as the normalized difference (ND). For two spectral bands, $A(x, y)$ and $B(x, y)$, the ND is computed as

$$ND_{AB}(x, y) = \frac{A(x, y) - B(x, y)}{A(x, y) + B(x, y)} \quad (1)$$

for each image pixel (x, y) . This concept was adapted for use with time series data, resulting in the GO ratio

$$GO(t) = \frac{F(t)_{515} - F(t)_{575}}{F(t)_{515} + F(t)_{575}} \quad (2)$$

where $F(t)_b$ represents fluorescence at sample point t in the time series ($-1 \leq GO(t) \leq 1$). The GO ratio accentuates the variance between the input signals. For highly correlated signals, this ratio will be relatively flat.

Results

A typical set of images corresponding to each of the fluorescent wavebands is depicted in Fig. 3. Initial inspection of the corrected images revealed two features of the data that would impact the analysis. First, both the 515 and 575 nm signals (Fig. 3A and 3B, respectively) emanated from the polyp centers with fluorescence values rapidly decreasing in the areas between polyps: fluorescence values dropped by 70–90% for the 515 pigment and by 60–80% for the 575 pigment. Salih et al. (1997) reported a similar concentration of fluorescent pigments around corallite rims and polyp centers. Chlorophyll fluorescence (Fig. 3C), however, was rather evenly distributed across the surface of the coral, except at the polyp centers where its intensity was diminished. Interestingly, this decline was considerably smaller, on the order of 10–30%. The other noteworthy attribute is that most of the corals exhibited uniform chlorophyll fluorescence across their entire surface (Fig. 4A–C). The fluorescence emissions were not static but appeared to evenly increase or decrease across the coral. The one outlier was treatment coral 4 (Fig.

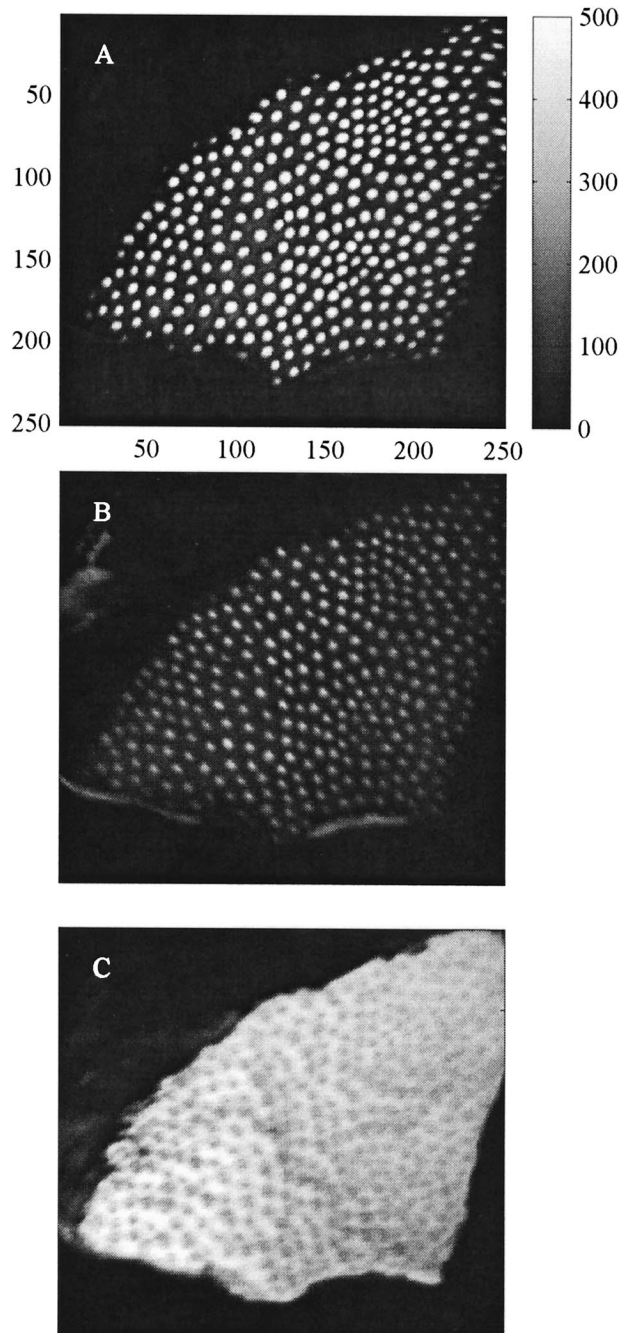


Fig. 3. Sample corrected coral fluorescence images. Given the high spatial resolution of the imagery, individual polyps are clearly visible. The images are from the (A) 515 nm, (B) 575 nm, and (C) 685 nm spectral bands of LUMIS. Each image is 11×11 cm (250×250 pixels) in size with a resolution of approximately $400 \mu\text{m}$ pixel⁻¹. The color bar scale is in digital numbers.

4D–F), in which bleaching emanated from one corner and gradually spread across its surface.

From these images, time series of average fluorescence were constructed for all pigments and corals (see *Materials and methods, image processing*). These series are presented in Fig. 5 (control corals) and Fig. 6 (treatment corals), where the three columns represent the 515, 575, and 685 nm fluo-

rescence values, respectively, and the rows contain the data for a given coral. The fluorescence values are reported in units of digital numbers (DN) recorded by the camera system. To help evaluate coral stress response, the temperature profile imposed on the treatment corals is shown above each column in Fig. 6. Plotted with each time series are the corresponding 99% confidence intervals. The small magnitude of the intervals is indicative of the precision of the fluorescence values. Such precise measurements are attributable to the high sensitivity, spatial resolution, and linearity of the LUMIS CCD camera.

Considering the overall strength of the fluorescence emissions reveals some interesting patterns. Recorded chlorophyll fluorescence is the strongest, followed by 515, then 575, which is roughly one-third as strong as 515. In terms of control versus treatment corals, the magnitude of chlorophyll fluorescence is roughly the same for both, excluding those that exhibited a stress-induced decline. For the 515 and 575 pigments, however, the control coral emissions generally are equal to or greater than their paired treatment counterparts. Over the course of the experiment, each coral exhibited considerable fluorescence variability with respect to both of these pigments. Among the control corals, a 56% difference between the weakest and strongest 515 emission was recorded for coral 7, while coral 5 had a 191% difference. For the 575 pigment, the control group showed changes from 36% (coral 7) to 106% (coral 3).

Of primary interest to this study was the behavior of animal pigment fluorescence in response to thermal stress relative to that of chlorophyll fluorescence, an accepted coral bleaching indicator. As evident from the control coral time series (Fig. 5, 685 nm column), chlorophyll fluorescence remained relatively constant, indicating the stability of the control corals. The treatment corals, however, displayed different reactions to thermal stress as noted by visual observations and supported by the response of chlorophyll fluorescence (Fig. 6, 685 nm column). Treatment corals 1–3 succumbed to the elevated temperatures and died. Noteworthy is the rapid response of these specimens to the second temperature spike. Within the resolution of our sampling frequency, the corals reacted to the applied stress within 12 h. Surprisingly, treatment corals 5–7 appeared immune to the thermal stress. Treatment coral 4 displayed an intermediate tolerance to temperature increases. Initially it declined, but it partially recovered and possibly acclimated to the 31°C water. The second temperature increase produced another drop in fluorescence, though less dramatic. Once the temperature was returned to baseline conditions, chlorophyll fluorescence rebounded to near initial levels.

In addition to exhibiting varied chlorophyll fluorescence responses, the corals contained a mixture of symbiotic dinoflagellates from three different clades (Table 2). The presence of *Symbiodinium* E in all of the surviving treatments is particularly interesting. This clade has been found predominantly in *Montastraea* spp. from coastal regions off Panama with environmentally stressful conditions (Toller et al. 2001).

The corresponding host pigment responses (515 and 575 nm columns in Figs. 5 and 6), by themselves, do not appear

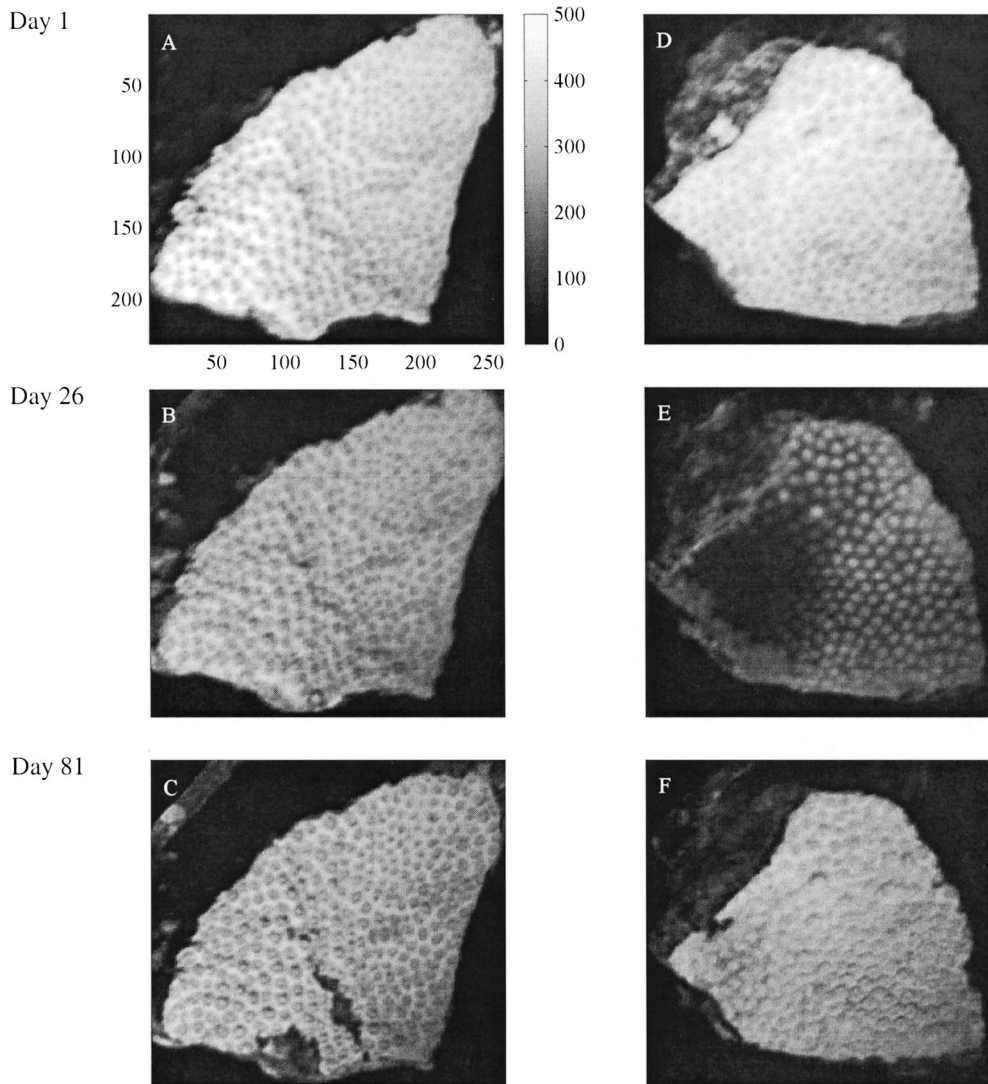


Fig. 4. Chlorophyll fluorescence of the control–treatment pair coral 4. The uniform fluorescence displayed by the control (A–C) was typical for most of the corals in this experiment. Even the treatment corals that bleached tended to do so in a uniform fashion. The one exception was treatment coral 4 (D–F), which exhibited more pronounced bleaching (less fluorescence) in the lower left (black) region. All the images are displayed with the same color map scale. Values are in digital numbers.

to reflect the same trends. In fact, these pigments show little, if any, correlation to the corresponding chlorophyll signal. In terms of absolute signal strength, 515 fluorescence is roughly $3\times$ greater than that at 575 and tends to exhibit greater variability among samples. This pattern holds for both the control and treatment corals, except for the three that died (treatments 1–3). In the time series for treatment corals 1–3, there is a point where the average 515 nm fluorescence falls below 575 nm fluorescence and gradually declines to zero. For corals 1 and 3, this crossover occurs before the second temperature spike, while it happens 24 h after this increase for coral 2 (Fig. 7).

To better illustrate the interplay between these two signals, the normalized difference or GO ratio for 515:575 was computed according to Eq. 2 on a temporal basis, yielding a

curve that agrees with chlorophyll fluorescence in terms of the final state of a given coral (Fig. 8).

Discussion

Instrumentation issues—In analyzing the fluorescence images, one should consider the significance of the major physical factors involved in image formation. The principal contributing factors to a recorded image (I) can be summarized mathematically as

$$I = F + D + S + N_F + N_D + N_R \quad (3)$$

where F is coral fluorescence, D is dark current, S is leakage, N_F is photon shot noise associated with the fluorescent signal, N_D is dark current noise, and N_R is readout noise attri-

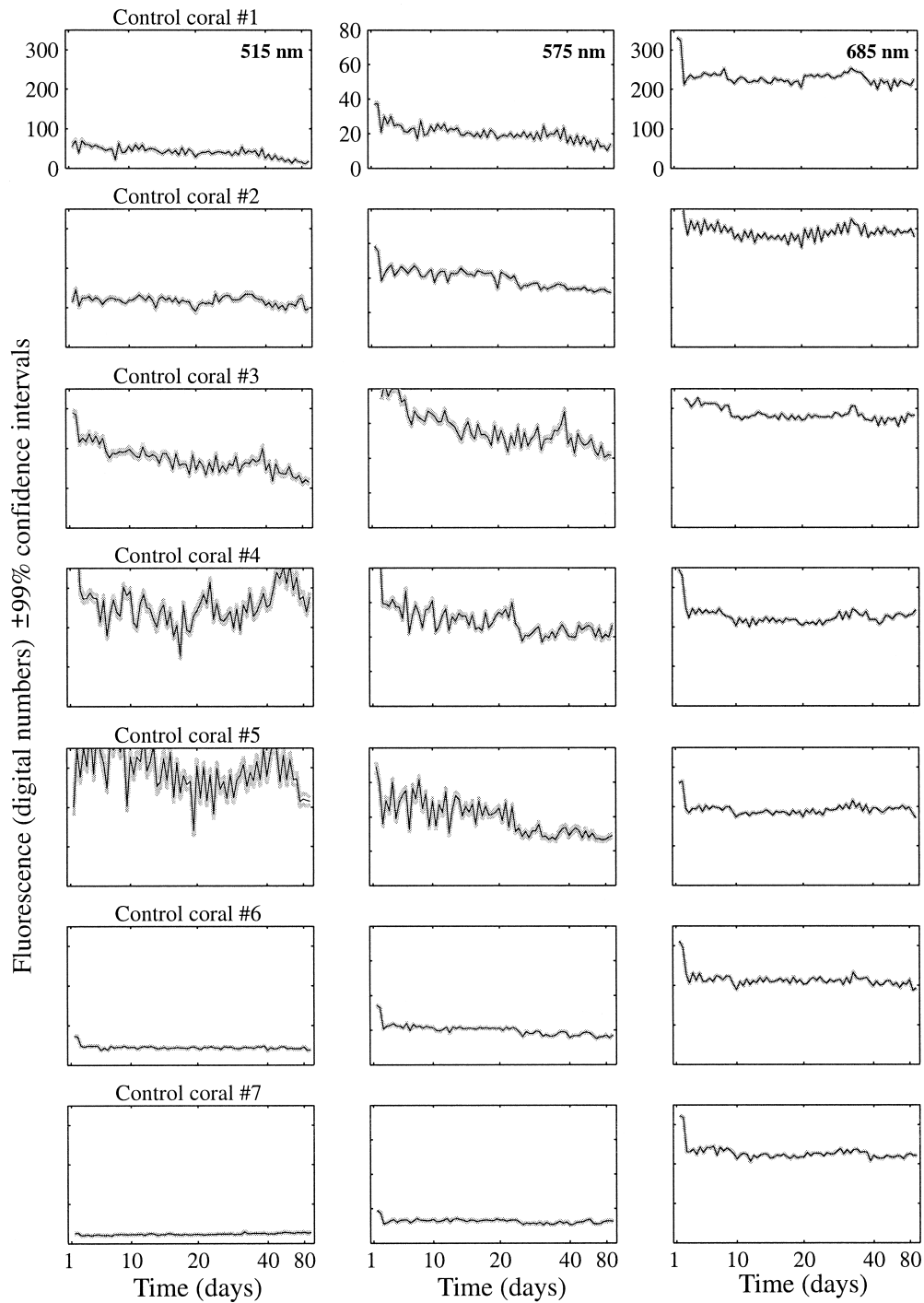


Fig. 5. Time series for control corals. The columns pertain to the 515, 575, and 685 nm fluorescent emissions, respectively. Each row represents a different coral specimen. The corresponding 99% confidence intervals are plotted for each time series.

buted to the electronic components of the camera. For this discussion, all of the terms are considered to be in units of digital numbers (DN) and the subscripts (x, y) denoting individual pixel locations have been omitted for clarity. In an ideal situation, the image would be an exact quantization of the fluorescent energy and Eq. 3 would reduce to $I = F$.

The dark current was easily quantified (*see Materials and*

methods, image correction) and subtracted from each pixel in a raw LUMIS image. Eliminating the effects of strobe leakage proved to be more difficult. While custom-made interference filters with excellent transmission and off-band rejection characteristics were used in LUMIS, it was not possible to attain absolute blockage outside of the filter passbands. To gauge the impact of this leakage on the fluores-

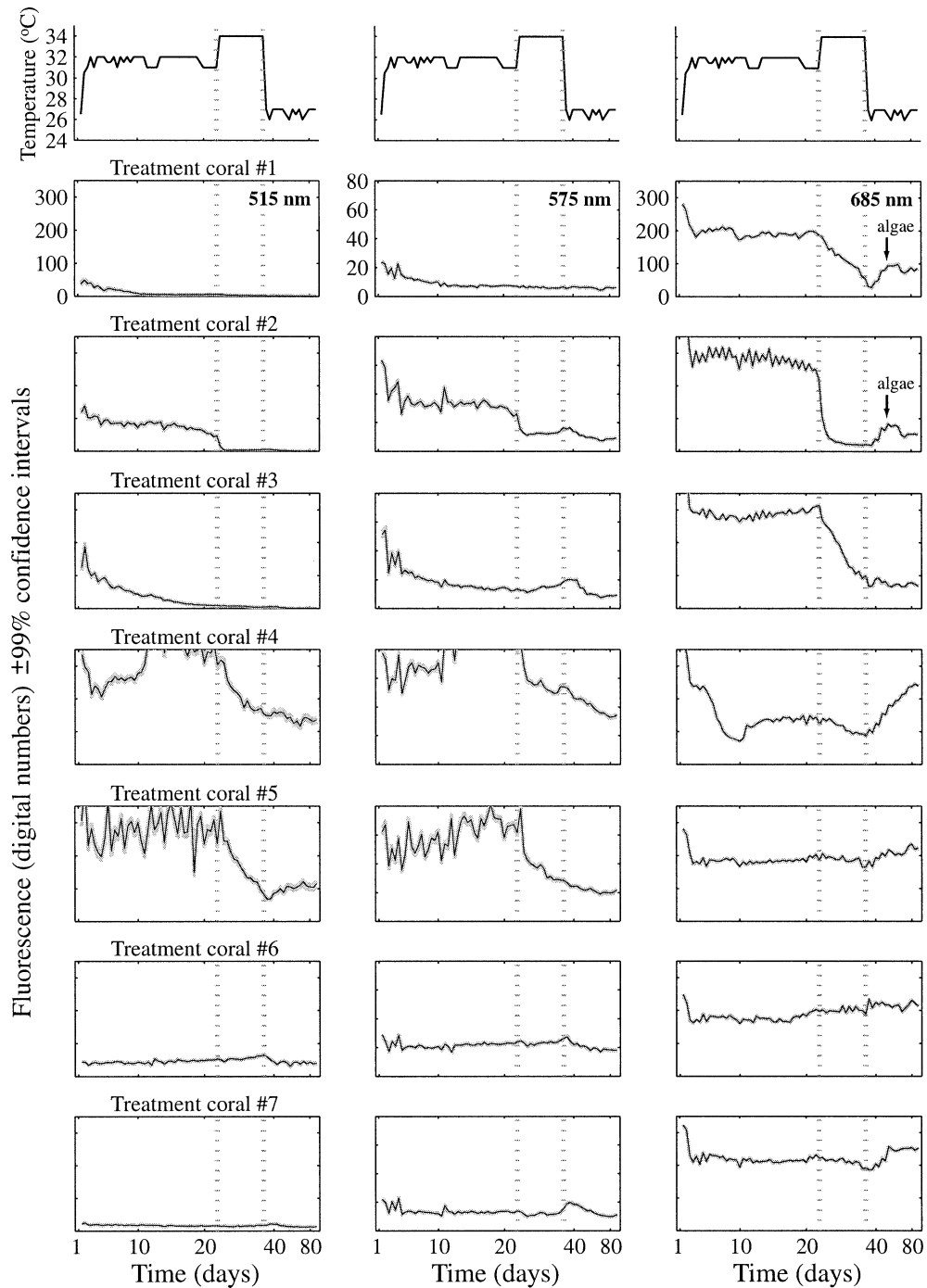


Fig. 6. Time series for treatment corals. The columns pertain to the 515, 575, and 685 nm fluorescent emissions, respectively. Each row represents a different coral specimen. The corresponding 99% confidence intervals are plotted for each time series. The temperature profile is plotted in the top row and repeated in each column for convenience. Arrows indicate an increase in 685 (chlorophyll) fluorescence attributable to filamentous algal growth on dead coral surfaces.

cence measurements, a computer model was developed for the experimental setup. Detailed specifications on camera performance and spectral transmission curves for the filters were obtained from the respective manufacturers and incorporated into the model. The strobe was assumed to have a

10% conversion efficiency throughout the visible spectrum (400–700 nm). The model indicated that strobe leakage could be responsible for 1–5 DN of measured signal, depending upon wavelength and surface characteristics of each coral. Any leaked light with wavelengths corresponding to

Table 2. Symbiotic dinoflagellate clades initially present in the coral specimens.

Specimen	Clade	Status
Coral 1	E	Died
Coral 2	A	Died
Coral 3	C	Died
Coral 4	C + E	Survived
Coral 5	E	Survived
Coral 6	E	Survived
Coral 7	E	Survived

the LUMIS fluorescence bands and reflected by a coral specimen would become intermixed with the targeted fluorescence signals. As a result, observed changes in the recorded fluorescence signals would contain a component associated with the reflection properties of the coral.

The remaining three terms pertain to noise sources in the measured signal for every pixel. Photon shot noise arises from the quantum nature of light. The number of photons striking a given pixel over any time interval varies randomly according to a Poisson distribution. This variability is an inherent characteristic of light that is quantified as the square root of the number of photoelectrons generated by the incident photon flux. The large pixel size and photon storage capacity (pixel full well depth) of the CCD camera in LUMIS help to minimize the impact of shot noise. Averaging N images together also reduces shot noise by the factor \sqrt{N} per pixel. The averaging steps used in processing the raw data served to reduce shot noise to less than 1 DN. Like shot noise, dark current noise derives from variability during the thermal generation of electrons in the CCD. For the camera

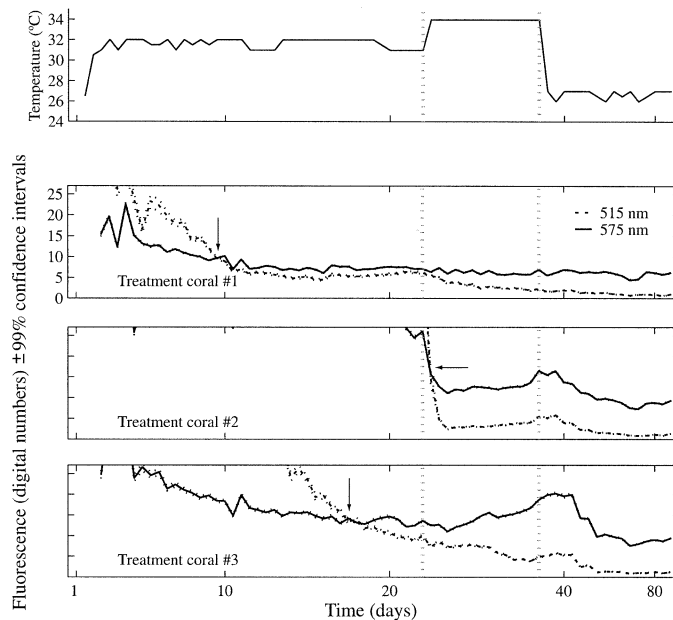


Fig. 7. Green–orange crossover. Each of the corals that died exhibited a shift in the dominance of the 515 over 575 pigment fluorescence either before or within 24 h of the second temperature increase. No other coral, control or treatment, displayed such a shift. Arrows denote the point of crossover.

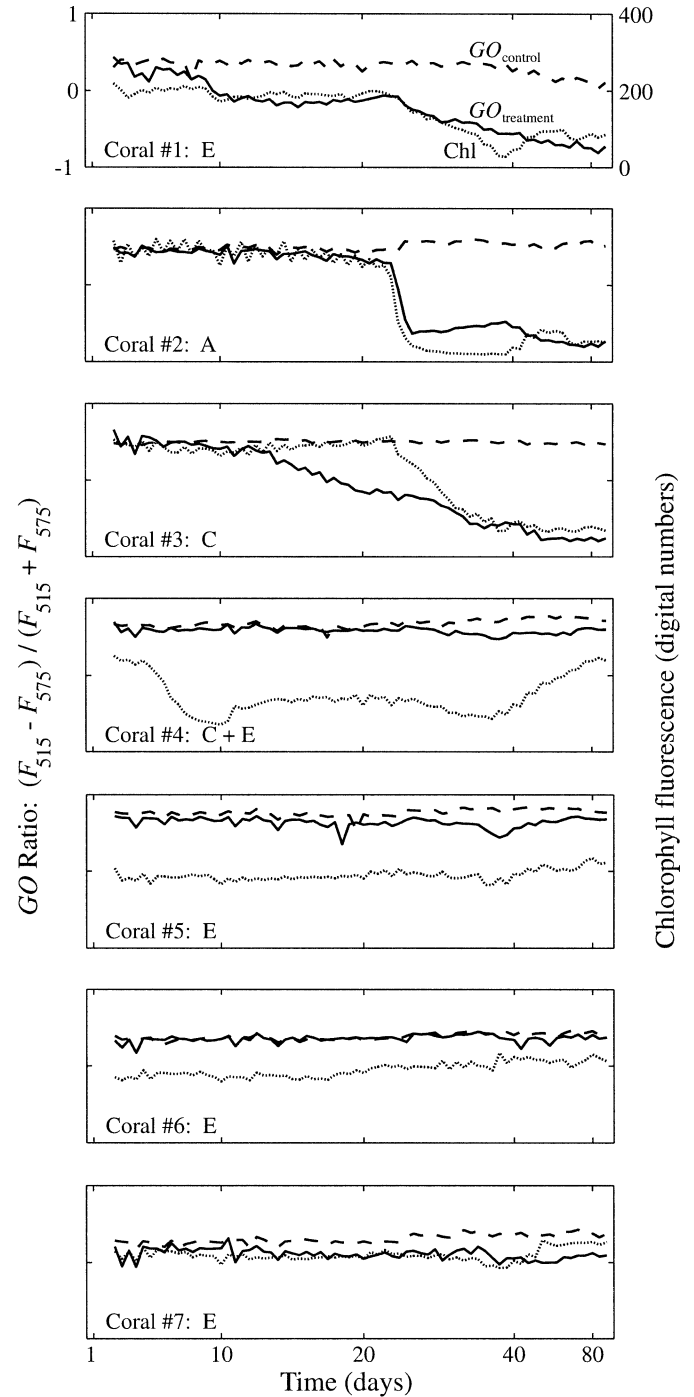


Fig. 8. The GO ratio. The normalized difference ratio of green (515 nm) to orange (575 nm) fluorescence is plotted for each of the seven coral pairs. The dashed line corresponds to the control and the solid line to the paired treatment coral. For comparison purposes, the chlorophyll fluorescence of the treatment coral is plotted as a dotted line. Letters in each plot designate symbiotic dinoflagellate clades present in the coral specimens.

system in LUMIS, this noise term is less than 1 DN for exposure times of less than 1 s. Readout noise collectively refers to the various sources of noise intrinsic to the electronic components in the camera system, especially the pre-amplifier. For low-light applications, the amount of readout noise is critical since it serves as the detection limit of the camera system. For LUMIS, readout noise is ≤ 15 electrons rms, which means that more than 15 photoelectrons must be collected by a pixel in order to record a meaningful signal. The LUMIS camera has a gain of 9 electrons DN^{-1} , so pixel values less than 2 DN are indistinguishable from noise. Fortunately, readout noise is also reduced by averaging images and for our study was less than 1 DN.

Being conservative, noise contributions do not pose a problem in this study as long as the recorded signal is ≥ 2 DN. Thus, the value at any image pixel is primarily a measure of fluorescence, with a possible small contribution from reflectance, and Eq. 3 may be simplified to $I = F + S$. While we cannot discount the possibility of reflected light contributing to the recorded signal, we favor the hypothesis that the primary origin of the light we measured was fluorescence. As bleaching progressed, the loss of pigmentation increased the albedo of the coral. Clear distinctions have been found between the reflectance spectra of healthy and bleached corals (Holden and LeDrew 1998). More importantly, over the spectral bands of interest in this study, reflectance has been observed to more than double for bleached corals (Myers et al. 1999). If reflected light were a major constituent in the present data set, then an increase in apparent fluorescence would be evident. The data, however, exhibit a declining trend as the corals bleached and/or died (Fig. 7). Our interpretation of the results, therefore, regards the observed changes to be a consequence of decreased pigment concentrations and/or fluorescence efficiencies.

Interpretation of numerical fluorescence values—Caution should be exercised with regard to interpreting the numerical results of this study. As stated in the Materials and methods section, the data in this study were not normalized to account for the spectral sensitivity characteristics of LUMIS. Individual results may vary, depending upon the properties of a particular imaging system. The important results are the observed trends in fluorescence, not the absolute magnitudes.

Distribution of the 515, 575, and 685 pigments—The fluorescence imagery revealed an inverse pattern between the spatial location of the host-based pigments and chlorophyll within the symbiotic dinoflagellates. Both the 515 and 575 fluorescent signals were strongest where chlorophyll fluorescence was weakest. Such an arrangement suggests a localization of the 515 and 575 pigments so as to minimize interference with light available for photosynthesis by the symbiotic dinoflagellates. This finding is inconsistent with reports that fluorescent pigments serve as UVA protectants for symbiotic dinoflagellates (Salih et al. 1997, 2000; Dove et al. 2001). If the primary function of the 515 and 575 pigments was to act as a sunscreen, one would expect maximal fluorescence values above regions coincident with high densities of symbiotic dinoflagellates. It is possible that these pigments afford some measure of protection to the gonads

of the coral (Salih et al. 1997), which lie beneath the regions of concentrated 515 and 575 fluorescence, but even this possibility is unlikely, based on spectral data. Characteristic excitation spectra measured by Mazel (1997a) indicate little activity in the UVA waveband. At least for *M. faveolata*, the role of photoprotectant seems doubtful for the 515 and 575 pigments. Perhaps the discrepancy is related to geographical (Caribbean vs. Pacific) and/or morphological (relatively smooth, expansive surface versus branching) differences between the respective corals under investigation. Also, in this study corals were subjected to a thermal stress under low irradiance levels. Given high irradiance conditions, the corals might disperse these pigments to shield the symbiotic dinoflagellates.

As an alternative interpretation, if symbiotic dinoflagellates overlie the 515 and 575 pigments, then the observed inverse pattern (Fig. 3) could be attributed to a masking effect. However, this scenario also seems improbable for several reasons. Recall the fluorescence differences between interpolyp valleys and polyp centers. Chlorophyll values dropped by 10–30%, while the animal pigments increased 70–90%. It is difficult to accept that the relatively small decrease in chlorophyll fluorescence over polyp centers could account for the dramatic increase in 515 and 575 fluorescence. Furthermore, such a distribution of pigments has only been reported for corals living in low-light habitats (Schlichter et al. 1986; Salih et al. 1997). More commonly, fluorescent pigments are situated in the outer ectodermal tissue of the coral (Kawaguti 1944; Mazel 1995, 1997a). Finally, images of *M. faveolata* from nearby patch reefs (2–3 m deep) taken in situ exhibited similar inverse patterns (Zawada unpubl. data). The animal pigments fluoresced more intensely in regions corresponding to weaker chlorophyll fluorescence.

Variability in chlorophyll fluorescence—In this study, chlorophyll fluorescence was used as a reference for evaluating the degree of coral bleaching. The recorded response of this signal was in agreement with visual observations made throughout the experiment. Inspection of this signal for the controls (Fig. 5) shows that these corals remained stable throughout the experiment. A linear least squares fit of the data indicated a small negative slope, which is not surprising given the length of the experiment and the sub-optimal laboratory conditions. When compared to the performance of identical treatment specimens, this decline is negligible. The behavior of the treatment corals (Fig. 6), however, was not as consistent. All of the corals were collected from the same small reef at approximately the same depth. Yet there is a high degree of intraspecific variability regarding the response to elevated temperatures. Corals 5–7 seemingly were unaffected by the 7°C increase in water temperature, while corals 1–3 succumbed after the second temperature increase. It should be pointed out that the rise in chlorophyll fluorescence for corals 1 and 2 during the final 40 d of the experiment does not indicate recovery. Rather, this increase is attributed to the growth of filamentous algae on the exposed coral skeletons (*see* arrows in Fig. 6). Coral 4 exhibited an intermediate response, declining rapidly from the start, then partially recovering, only to decline again after

the second temperature increase, and, finally, recovering to near its initial state once water temperatures were returned to normal. Such intraspecific differences in susceptibility to thermal stress have been reported for Caribbean and Pacific corals (Jokiel and Coles 1977; Gates 1990; Szmant and Gassman 1990; Jones 1997) and suggest an ability to tolerate higher temperatures (Brown 1997a) in some but not all corals.

This variability also raises the question of the importance of the types of symbiotic dinoflagellates harbored by the corals. Based on genetic analysis, most coral symbionts can be assigned to one of three common clades of *Symbiodinium*: A, B, or C (Rowan and Powers 1991). A fourth distinct taxon, *Symbiodinium* E, has recently been identified in corals belonging to the *Montastraea* species complex (Toller et al. 2001). In the Caribbean sibling species *Montastraea annularis* and *M. faveolata*, Rowan and Knowlton (1995) found that A and B were the dominant genotypes in specimens of both corals collected from depths less than 6 m, while only C existed in specimens below 9 m. Mixtures of C with A and/or B were common at intermediate depths. Such depth zonation, they concluded, supports the hypothesis that the type of symbiotic dinoflagellate plays a functional role in the adaptability of the coral. Further work (Rowan et al. 1997) has revealed that the diversity and zonation of symbiotic dinoflagellates in *M. annularis* and *M. faveolata* account for intraspecific variability in bleaching patterns. In concert with symbiont polymorphism, host genotypic variations may also contribute to these patterns (Edmunds 1994).

Genetic analysis disclosed that the corals in this study contained an odd mixture of symbiotic dinoflagellates (Table 2). Interestingly, all the corals that survived the heat stress contained *Symbiodinium* E, while two of the dead corals did not contain any *Symbiodinium* E. The one outlier is treatment coral 1, which primarily harbored *Symbiodinium* E, but nevertheless died. This clade is locally abundant in coastal regions off Panama near river outflows (Toller et al. 2001). It is hypothesized that this clade contributes to the heartiness of the corals living in these habitats by tolerating environmental conditions inhospitable to other taxa of symbiotic dinoflagellates. *Symbiodinium* E is uncommon in offshore reefs and in the Bahamas (N. Knowlton, Scripps Institution of Oceanography, pers. comm.). Perhaps the presence of this clade is responsible for the thermal tolerance exhibited by treatment specimens 4–7.

Correlation between the 515 and 575 signals—The primary goal of this study was to investigate the potential utility of the 515 and 575 nm fluorescent pigments as alternative proxies for coral stress. The experimental responses of these two pigments for the control and treatment corals (Figs. 5 and 6, respectively) reveal several interesting patterns: (1) Prior to bleaching, the 515 nm emission is stronger than that at 575 nm. However, the intensity of these emissions varies from coral to coral. Compare this behavior with that of chlorophyll fluorescence, where the emissions are the same order of magnitude for all corals until the onset of bleaching. (2) For those treatment corals that died, the 515 and 575 nm emissions for the controls were higher than those of the cor-

responding paired treatments throughout the experiment. This response could be attributable to these animal pigments possibly being more sensitive stress indicators. (3) To a first order, the 515 and 575 nm emissions appear to be highly correlated. One explanation is leakage of the 515 signal. The 515 emission is very broad and can spill over into the emission range for 575 (Mazel 1997a), so it is possible that some of the 575 signal is attributable to 515. For the bleaching corals of this study, however, such an explanation collapses prior to the second temperature increase. From day 22 through the end of the experiment, the 575 emission is greater than the 515 emission. Plots of 515 and 575 fluorescence with their respective 99% confidence intervals (Fig. 7), which are less than 1 DN in magnitude, show the absence of overlap between these intervals. A two-sample, two-tailed *t* test (Zar 1999) confirmed the statistical significance of this difference.

These characteristics further cast doubt on a photoprotective role for the 515 and 575 pigments. In that capacity, the pigments would be expected to manifest a relatively constant fluorescence response in both spatial and temporal contexts. Additionally, it is interesting that there is no apparent relationship between fluorescence intensity and resistance to bleaching. The most resilient corals might be expected to have more efficient sunblockers and, consequently, higher 515 and 575 fluorescence values. But, consider coral pairs 6 and 7. The controls have the weakest 515 and 575 emissions (Fig. 5), yet the corresponding treatments exhibited no signs of bleaching. Contrast this response with the bleaching coral 3, for which the paired control had relatively strong fluorescent emissions.

GO ratio—Given the independence of the 515 and 575 signals, the question still remains regarding a correlation with coral bleaching. Separately, there does not appear to be any correspondence between either of them and chlorophyll fluorescence, our chosen bleaching indicator. However, taking the normalized difference ratio (Eq. 2) of green (515 nm) to orange (575 nm), fluorescence (GO) reveals the underlying uniqueness of these signals. The GO ratio is plotted as a function of time in Fig. 8 for each coral. The dashed line represents the control and the solid black line the paired treatment coral. For comparison purposes, chlorophyll fluorescence for the treatment is also plotted as the dotted line. The first noteworthy point is the correspondence to chlorophyll fluorescence. For both the controls and those treatments that survived the heat stress, the GO ratio remains relatively flat; for those corals that died, it drops and remains between -1 and 0 . What is intriguing about this behavior of the GO ratio is that it is based on pigments residing in the animal tissue and not the symbiotic dinoflagellates.

While the end results of the GO ratio and chlorophyll fluorescence are the same, i.e., both clearly indicate coral death or survival, there are some differences. For example, in corals 1 and 3 the GO ratio declines about 10 d prior to chlorophyll fluorescence (Fig. 8). For coral 4, the GO ratio remains stable throughout the experiment, while chlorophyll fluorescence experiences several declines and recoveries. We speculate that such inconsistencies are caused by the different origins of the pigments. The 515 and 575 pigments are

believed to be animal-based, while chlorophyll is plant-based. It is possible that the particular symbiotic dinoflagellates in coral 4 were more thermally sensitive.

Another interesting issue regarding the GO ratio is its underlying meaning. For the three dead corals, there is a point in time when the 515 signal drops below the 575 signal. Why does the 515 pigment decline more extensively or, conversely, why does the 575 pigment appear to be more robust? There is some spectral evidence suggesting that phycoerythrin is responsible for the 575 nm signal (Kawaguti 1944; Mazel 1997a). If this pigment is indeed phycoerythrin, it raises the specter of the corals hosting a second symbiont, possibly a type of cyanobacteria. The difference, then, could be attributed to the individual thermal tolerances of the coral animal, the symbiotic dinoflagellates, and the cyanobacteria.

It is not unreasonable to expect different organisms to react differently to elevated temperatures. In both plants and animals, thermal stress induces the production of heat shock proteins (HSPs) that help protect against thermal damage and assist in recovery on the cellular level (Parsell and Lindquist 1993). Synthesis of HSPs occurs at different temperatures in different organisms (Parsell and Lindquist 1993). A number of HSPs have been identified in various species of coral (Black et al. 1995; Hayes and King 1995; Fang et al. 1997; Sharp et al. 1997), symbiotic dinoflagellates (Downs et al. 2000), and cyanobacteria (Borbely and Suranyi 1988; Eriksson and Clarke 1996; Roy et al. 1999).

Several recent studies have addressed the production of HSPs in corals and their algal symbionts. In both *M. faveolata* (Black et al. 1995; Downs et al. 2000) and *Goniopora djiboutiensis* (Sharp et al. 1997), significant HSP induction was not detected until the corals were exposed to water temperatures of 33°C or higher. Importantly, photosynthesis in cultured symbiotic dinoflagellates from the jellyfish *Cassiopeia xamachana* becomes impaired at temperatures above 30°C and completely ceases around 34°C (Iglesias-Prieto et al. 1992). These findings indicate a heightened thermal sensitivity in the algae, compared with that of the coral. Additionally, HSP production was determined to be regulated by environmental conditions. Production increased in proportion to the severity of the thermal stress.

In contrast to the symbiotic dinoflagellates, cyanobacteria exhibit higher levels of thermotolerance. HSPs provide protection for the photosynthetic apparatus of these organisms to temperatures as high as 50°C (Eriksson and Clarke 1996; Nakamoto et al. 2000). If corals harbor cyanobacteria, then this evidence supports the interpretation of the GO ratio as a manifestation of the differential thermotolerances of the coral animal and this new symbiont.

In terms of utility, the GO ratio has the advantage of being immune to interference by chlorophyll fluorescence from other sources. Recall the increase in chlorophyll fluorescence for corals 1 and 2 over the last 40 d of the experiment (Fig. 8). This signal is attributed to filamentous algal growth atop the dead corals. The GO ratio continues to decline during this time.

In this study, high-resolution multispectral imagery was employed to investigate the fluorescent responses of two host-based pigments, plus chlorophyll, during a thermally induced bleaching process. Analysis of the data disclosed

both spatial and temporal patterns. The imagery revealed that fluorescent emissions of both the green and orange host pigments were concentrated at polyp centers and declined by 70–90% in regions between polyps. In contrast to these pigments, chlorophyll fluorescence was more uniform, decreasing by only 10–30% around polyp centers. This distribution of the host-based pigments is consistent with the hypothesis that these compounds may provide some measure of photoprotection to the coral reproductive organs. However, the results do not support the proposition that these pigments function as a sunscreen for the symbiotic dinoflagellates.

Temporal analysis demonstrated that the GO ratio, the normalized difference ratio of green (515 nm) to orange (575 nm) fluorescence, can be used as an additional indicator of coral bleaching. Moreover, a sustained GO ratio of less than zero seems to signal impending coral death. Finally, an advantage of the GO ratio is resistance to contamination from other sources of chlorophyll fluorescence, such as filamentous algae.

References

- BLACK, N. A., R. VOELLMY, AND A. M. SZMANT. 1995. Heat shock protein induction in *Montastraea faveolata* and *Aiptasia pallida* exposed to elevated temperatures. *Biol. Bull.* **188**: 234–240.
- BORBELY, G., AND G. SURANYI. 1988. Cyanobacterial heat-shock proteins and stress responses. *Methods Enzymol.* **167**: 622–629.
- BROWN, B. E. 1997a. Adaptations of reef corals to physical environmental stress. *Adv. Mar. Biol.* **31**: 221–299.
- . 1997b. Coral bleaching: Causes and consequences. *Coral Reefs* **16**: S129–S138.
- CATALA, R. 1959. Fluorescence effects from corals irradiated with ultra-violet rays. *Nature* **183**: 949.
- DELBEEK, J. C., AND J. SPRUNG. 1994. The reef aquarium: A comprehensive guide to the identification and care of tropical marine invertebrates, 1st ed. Ricordea.
- DOVE, S. G., O. HOEGH-GULDBERG, AND S. RANGANATHAN. 2001. Major colour patterns of reef-building corals are due to a family of GFP-like proteins. *Coral Reefs* **19**: 197–204.
- DOWNS, C. A., E. MUELLER, S. PHILLIPS, J. E. FAUTH, AND C. M. WOODLEY. 2000. A molecular biomarker system for assessing the health of coral (*Montastraea faveolata*) during heat stress. *Mar. Biotechnol.* **2**: 533–544.
- EDMUNDS, P. J. 1994. Evidence that reef-wide patterns of coral bleaching may be the result of the distribution of bleaching-susceptible clones. *Mar. Biol.* **121**: 137–142.
- ERIKSSON, M.-J., AND A. K. CLARKE. 1996. The heat shock protein clpb mediates the development of thermotolerance in the cyanobacterium *Synechococcus* sp. Strain pcc 7942. *J. Bacteriol.* **178**: 4839–4846.
- FANG, L.-S., S.-P. HUANG, AND K.-L. LIN. 1997. High temperature induces the synthesis of heat-shock proteins and the elevation of intracellular calcium in the coral *Acropora grandis*. *Coral Reefs* **16**: 127–131.
- FITT, W. K., AND M. E. WARNER. 1995. Bleaching patterns of four species of Caribbean reef corals. *Biol. Bull.* **189**: 298–307.
- GATES, R. D. 1990. Seawater temperature and sublethal coral bleaching in Jamaica. *Coral Reefs* **8**: 193–197.
- GLYNN, P. W. 1993. Coral reef bleaching: Ecological perspectives. *Coral Reefs* **12**: 1–17.

- . 1996. Coral reef bleaching: Facts, hypotheses and implications. *Glob. Chang. Biol.* **2**: 495–509.
- GREEN, W. B., P. L. JEPSEN, J. E. KREZNAR, R. M. RUIZ, A. A. SCHWARTZ, AND J. B. SEIDMAN. 1975. Removal of instrument signature from Mariner 9 television images of Mars. *Appl. Opt.* **14**: 105–114.
- HARDY, J. T., F. E. HOGE, J. K. YUNGEL, AND R. E. DODGE. 1992. Remote detection of coral “bleaching” using pulsed-laser fluorescence spectroscopy. *Mar. Ecol. Prog. Ser.* **88**: 247–255.
- HAYES, R. L., AND C. M. KING. 1995. Induction of 70-kd heat shock protein in scleractinian corals by elevated temperature: Significance for coral bleaching. *Mol. Mar. Biol. Biotechnol.* **4**: 36–42.
- HOLDEN, H., AND E. LEDREW. 1998. Spectral discrimination of healthy and non-healthy corals based on cluster analysis, principal components analysis, and derivative spectroscopy. *Remote Sens. Environ.* **65**: 217–224.
- IGLESIAS-PRIETO, R., J. L. MATTA, W. A. ROBINS, AND R. K. TRENCH. 1992. Photosynthetic response to elevated temperature in the symbiotic dinoflagellate *Symbiodinium microadriaticum* in culture. *Proc. Natl. Acad. Sci. U.S.A.* **89**: 10302–10305.
- JEFFREY, S. W., AND F. T. HAXO. 1968. Photosynthetic pigments of symbiotic dinoflagellates (zooxanthellae) from corals and clams. *Biol. Bull.* **135**: 149–165.
- JOKIEL, P. L., AND S. L. COLES. 1977. Effects of temperature on the mortality and growth of Hawaiian reef corals. *Mar. Biol.* **43**: 201–208.
- JONES, R. J. 1997. Changes in zooxanthellar densities and chlorophyll concentrations in corals during and after a bleaching event. *Mar. Ecol. Prog. Ser.* **158**: 51–59.
- KAUTSKY, H., AND A. HIRSCH. 1931. Neue versuche zur kohlen-säureassimilation. *Naturwissenschaften* **19**: 964.
- KAWAGUTI, S. 1944. On the physiology of reef corals: VI. Study on the pigments. *In* Palao tropical biological station studies. The Japan Society for the Promotion of Scientific Research.
- . 1969. Effect of the green fluorescent pigment on the productivity of the reef corals. *Micronesia* **5**: 313.
- . 1973. Electron microscopy on symbiotic algae in reef corals. *Publ. Seto Mar. Biol. Lab.* **20**: 779–783.
- LAZAR, D. 1999. Chlorophyll *a* fluorescence induction. *Biochem. Biophys. Acta* **1412**: 1–28.
- LILLESAND, T. M., AND R. W. KIEFER. 1994. Remote sensing and image interpretation, 3rd ed. Wiley.
- LIMBAUGH, C., AND W. J. NORTH. 1956. Fluorescent, benthic, Pacific coast coelenterates. *Nature* **178**: 497–498.
- LORENZEN, C. 1966. A method for the continuous measurement of *in vivo* chlorophyll concentration. *Deep-Sea Res.* **13**: 223–227.
- MAZEL, C. H. 1995. Spectral measurements of fluorescence emission in Caribbean cnidarians. *Mar. Ecol. Prog. Ser.* **120**: 185–191.
- . 1997a. Coral fluorescence characteristics: Excitation–emission spectra, fluorescence efficiencies, and contribution to apparent reflectance. Society of Photo-optical Instrumentation Engineers (SPIE) Proceedings **2963**: 240–245.
- . 1997b. Diver-operated instrument for *in situ* measurement of spectral fluorescence and reflectance of benthic marine organisms and substrates. *Opt. Eng.* **36**: 2612–2617.
- MOHAMMED, G. H., W. D. BINDER, AND S. L. GILLIES. 1995. Chlorophyll fluorescence—a review of its practical forestry applications and instrumentation. *Scand. J. For. Res.* **10**: 383–410.
- MYERS, M. R., J. T. HARDY, C. H. MAZEL, AND P. DUSTAN. 1999. Optical spectra and pigmentation of Caribbean reef corals and macroalgae. *Coral Reefs* **18**: 179–186.
- NAKAMOTO, H., N. SUZUKI, AND S. K. ROY. 2000. Constitutive expression of a small heat-shock protein confers cellular thermotolerance and thermal protection to the photosynthetic apparatus in cyanobacteria. *FEBS Lett.* **483**: 169–174.
- ONEILL, R. A., A. R. DAVIS, H. G. GROSS, AND J. KRUISS. 1975. A remote sensing laser fluorometer, p. 173–196. *In* Hongsuk H. Kim and Philip T. Ryan [eds.], The use of lasers for hydrographic studies. Proc. Symp. Wallops Flight Center, Wallops Island, Virginia. Scientific and Technical Information Office, National Technical Information Service. NASA SP 375 SRLF D0005324553.
- PARSELL, D. A., AND S. LINDQUIST. 1993. The function of heat-shock proteins in stress tolerance: Degradation and reactivation of damaged proteins. *Annu. Rev. Genet.* **27**: 437–496.
- PERRY, C., AND L. F. LAUTENSCHLAGER. 1984. Functional equivalence of spectral vegetation indices. *Remote Sens. Environ.* **14**: 169–182.
- PORTER, J. W., W. K. FITT, H. J. SPERO, C. S. ROGERS, AND M. W. WHITE. 1989. Bleaching in reef corals—physiological and stable isotopic responses. *Proc. Natl. Acad. Sci. U.S.A.* **86**: 9342–9346.
- ROWAN, R., AND N. KNOWLTON. 1995. Intraspecific diversity and ecological zonation in coral-algal symbiosis. *Proc. Natl. Acad. Sci. U.S.A.* **92**: 2850–2853.
- , ———, A. BAKER, AND J. JARA. 1997. Landscape ecology of algal symbionts creates variation in episodes of coral bleaching. *Nature* **388**: 265–269.
- , AND D. A. POWERS. 1991. A molecular genetic classification of zooxanthellae and the evolution of animal-algal symbioses. *Science* **251**: 1348–1351.
- ROY, S. K., T. HIYAMA, AND H. NAKAMOTO. 1999. Purification and characterization of the 16-kda heat-shock-responsive protein from the thermophilic cyanobacterium *Synechococcus vulcanus*, which is an alpha-crystallin-related, small heat shock protein. *Eur. J. Biochem.* **262**: 406–416.
- SALIH, A., O. HOEGH-GULDBERG, AND G. COX. 1997. Photoprotection of symbiotic dinoflagellates by fluorescent pigments in reef corals, p. 217–230. *In* Australian Coral Reef Society 75th Anniversary Conference.
- , A. LARKUM, G. COX, M. KUHL, AND O. HOEGH-GULDBERG. 2000. Fluorescent pigments in corals are photoprotective. *Nature* **408**: 850–853.
- SCHLICHTER, D., H. W. FRICKE, AND W. WEBER. 1986. Light harvesting by wavelength transformation in a symbiotic coral of the red sea twilight zone. *Mar. Biol.* **91**: 403–408.
- , U. MEIER, AND H. W. FRICKE. 1994. Improvement of photosynthesis in zooxanthellate corals by autofluorescent chromatophores. *Oecologia* **99**: 124–131.
- SHARP, V. A., B. E. BROWN, AND D. MILLER. 1997. Heat shock protein (hsp 70) expression in the tropical reef coral *Goniopora djiboutiensis*. *J. Therm. Biol.* **22**: 11–19.
- SHIBATA, K. 1969. Pigments and a UV-absorbing in corals and a blue-green alga living in the Great Barrier Reef. *Plant Cell Physiol.* **10**: 325–335.
- SZMANT, A. M., AND N. J. GASSMAN. 1990. The effects of prolonged “bleaching” on the tissue biomass and reproduction of the reef coral *Montastrea annularis*. *Coral Reefs* **8**: 217–224.
- TOLLER, W. W., R. ROWAN, AND N. KNOWLTON. 2001. Zooxanthellae of the *Montastraea annularis* species complex: Patterns of distribution of four taxa of *Symbiodinium* on different reefs and across depths. *Biol. Bull.* **201**: 348–359.
- ZAR, J. H. 1999. Biostatistical analysis, 4th ed. Prentice Hall.

Received: 17 September 2001

Accepted: 16 April 2002

Amended: 6 May 2002